Mediterranean Journal of Medicine & Medical Sciences
ISSN: 3107-2720
Mediterr J Med Med Sci
doi: 10.5281/zenodo.18667523
https://mmj.org.ly

SHORT COMMUNICATION article

Immune profile score of modified Tremelimumab with CTLA-4 could enhance immunotherapy using molecular docking

Najla A. Ieban [1], **Halima A. Gbaj** [2], **Mohamed A. Gbaj** [3]
Anton Hermann [4], and **Abdul M. Gbaj** [1 *]

[1] Department of Medicinal Chemistry, Faculty of Pharmacy, University of Tripoli, Tripoli, Libya
[2] Department of Microbiology and Immunology, Faculty of Pharmacy, University of Tripoli, Tripoli, Libya
[3] Department of Chemical Engineering, Faculty of Engineering, University of Tripoli, Tripoli, Libya
[4] Department of Biosciences, University of Salzburg, Salzburg, Austria
[*] Author to whom correspondence should be addressed

Received: 18-12-2025, **Accepted:** 15-02-2026, **Published online:**18-02-2026

HOW TO CITE THIS
Ieban et al. Immune profile score of modified Tremelimumab with CTLA-4 could enhance immunotherapy using molecular docking. Mediterr J Med Med Sci. 2026; 2(1): 40-50. [Article number: 25]. https://doi.org/10.5281/zenodo.18667523

Keywords: Antitumor immune response, docking, CTLA-4, epigenetic, genetic, Tremelimumab

Abstract: Cancer remains a leading cause of death worldwide and arises from genetic and epigenetic alterations that disrupt normal cellular regulation. Immune checkpoint pathways, particularly those involving CTLA-4, play a crucial role in suppressing antitumor immune responses. Immune checkpoint inhibitors such as Tremelimumab have revolutionized cancer therapy by restoring T-cell activity. Improving antibody-receptor interactions through molecular modification may further enhance therapeutic outcomes. Computational approaches such as molecular docking offer valuable tools for studying protein-protein interactions and guiding antibody optimization. The three-dimensional structure of the CTLA-4 receptor was obtained from the Protein Data Bank and prepared through energy minimization. The Tremelimumab antibody was modeled and modified at selected binding regions. Molecular docking simulations were performed to evaluate the interactions between the antibody and receptor. Docking complexes were analyzed for binding affinity, hydrogen bonding, and hydrophobic interactions using molecular visualization tools. Docking results demonstrated stable binding between modified Tremelimumab and CTLA-44. Certain modifications resulted in improved binding affinity, indicated by lower docking energy scores and enhanced interaction networks. Other modifications negatively affected binding due to steric hindrance or loss of key interactions. The study highlights the importance of antibody structure in determining immune checkpoint binding efficiency. Enhanced binding affinity may improve CTLA-4 blockade and strengthen antitumor immune responses. Molecular docking proved effective in predicting interaction patterns, though experimental validation is necessary to confirm biological relevance. This study aims to demonstrate that molecular modification of Tremelimumab can influence its interaction with CTLA-4.

Introduction

Cancer is considered one of the major global health problems due to its notable social and economicburden [1]. Cancer is defined as a wide range of diseases characterized by the loss of normal cellular regulation, leading to uncontrolled cell proliferation, evasion of programmed cell death, and the ability to invade surrounding tissues

and metastasize to distant organs [2]. Immunotherapy for cancer, often referred to as biological cancer treatment, involves the strategic modulation of the patient's immune responses to identify and eliminate malignant cells. Rather than relying solely on external therapeutic interventions, this approach emphasizes the development of agents that stimulate or amplify the immune system's ability to detect and eradicate neoplastic cells [3, 4]. The objective of the method is to enhance immunological responses, enabling the body to generate a more robust and targeted defense against tumor progression [5]. One of these approaches targets immune checkpoints directly, specifically by blocking the interactions between cytotoxic T-lymphocyte-associated protein 4 (CTLA-4) or programmed cell death protein 1 and their respective ligands, B7 or PD-L1 [5].CTLA4 (CD152) is a receptor found on the surface of activated T cells [6]. For a T cell to be fully activated, it needs two signals: First, a T cell receptor recognizing an antigen presented by the major histocompatibility complex on antigen-presenting cells (APCs), and second, the interaction between CD28 on the T cell and B7 family proteins (like B7.1/CD80, B7.2/CD86, B7-H3, and B7-H4) on the APCs. After the T cell is activated, it starts to express more CTLA4 on its surface. CTLA4 is similar to CD28, but it binds more strongly to B7 molecules. Because of this stronger binding, CTLA4 takes over and blocks CD28 from connecting with B7, which stops the second activation signal and reduces T cell activity [7].

Tremelimumab (previously known as ticilimumab) is a fully human monoclonal antibody of the IG2 type [6], composed of two identical heavy chains and two identical light chains, connected by disulfide bonds, targeting CTLA-4 receptors, proteins found on T cells, also helping in boostinginterleukin-2 (IL-2) activity. Pfizer company developed this antibody as a cancer treatment, originally created using Xeno Mouse technology from Abgenix (now part of Amgen) [6]. Tremelimumab is used intravenously with durvalumab, in a STRIDE regimen (Single Tremelimumab Regular Interval Durvalumab [8]. When Tremelimumab is combined with durvalumab, platinum-based chemotherapy is considered as first-line treatment for metastatic non-small lung cancer (mNSCLC) [9]. Monoclonal antibodies (mAbs) that target CTLA4 can block it from binding with B7 molecules on antigen-presenting cells (APCs). This stops the usual downregulation of T cell activity (**Figure 1**).

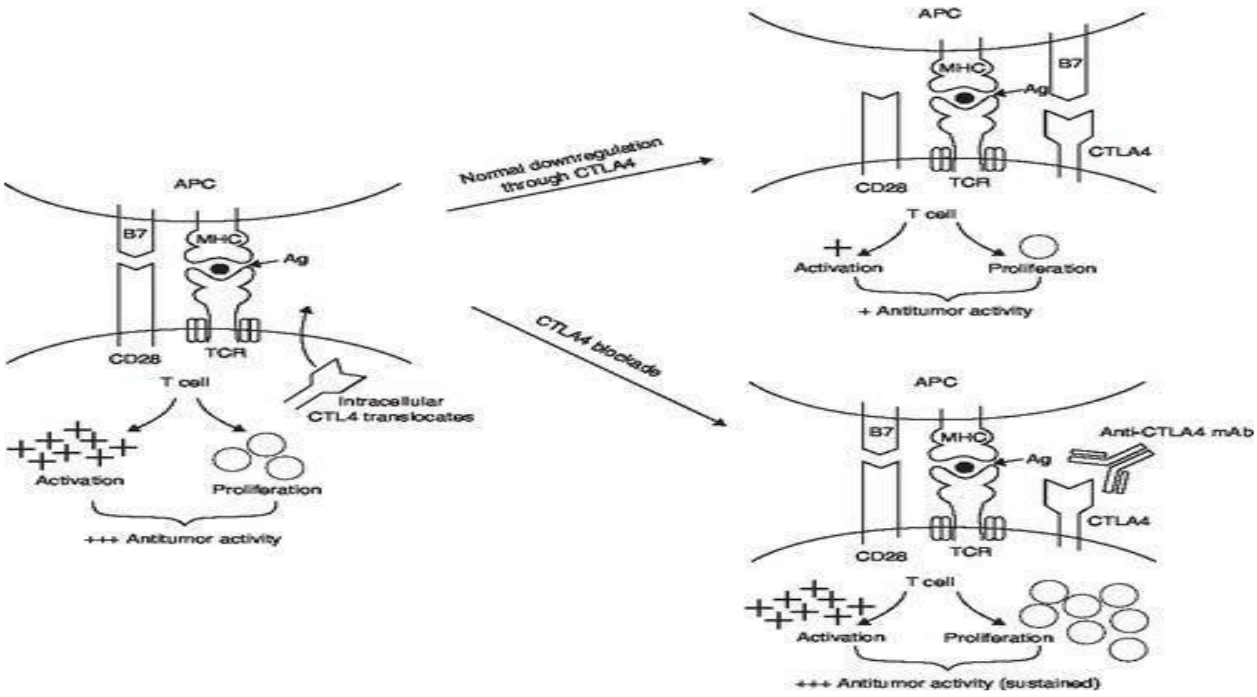

Figure 1: Blockade of cytotoxic T lymphocyte-associated antigen 4 (CTLA4) can prolong T-cell activation

Ag: Antigen; APC: Antigen-presenting cell; CTLA4: Cytotoxic T lymphocyte-associated antigen 4; mAb: Monoclonal antibody; MCH: Major histocompatibility complex; TCR: T-cell receptor [7]

When the CTLA4-B7 signal is blocked, T cells stay active for longer and work better. This can be observed through higher levels of cytokines like IL-2, IFN-γ, IL-3, IL-4, IL-5, and IL-10. Studies have tested this idea in mouse models using antibodies against mouse CTLA4, and the results showed stronger T cell responses and more efficient elimination of solid tumors like fibrosarcoma, colon cancer, and prostate cancer [7]. The aim of this study is to examine the binding interaction between Tremelimumab and the CTLA4 receptor through molecular docking methods. In addition, this study explores how specific modifications in the amino acid sequence of Tremelimumab may alter its binding affinity. By analyzing the original and altered sequences of Tremelimumab, this study attempts to better understand how minor adjustments at the molecular level can influence antibody function. It is hoped that the results will offer valuable information for future improvements in immune-based therapies for cancer.

Materials and methods

Molecular modeling tools: Tremelimumab and the CTLA4 receptor were obtained from PDB [10]. Visualized and modified via PyMOL [11], and PDBsum were used to illustrate the residues responsible for interaction between the receptor and ligand [12, 13].

Molecular docking: The receptor and the ligand were excluded from water molecules, the identical chains from the receptor and the ligand, leaving a single chain for the receptor and a single arm for the ligand. The hydrogen atoms were added, the ligand was modified at residues crucial for binding to the receptor, and at the end, the file was saved in PDB form. The docking process is done by Cluspro 2.0 server [14, 15].

Antibody developability: The allergenicity is predicted based on the amino acid sequence of the protein via AlgPred [16]. Antigenic Peptide Prediction Tool -Immuno-medicine Group is a tool designed to identify potential antigenic regions within protein sequences [17]. While the protparam tool is used to estimate some of the physicochemical properties, like the half-life and instability index [18]. Finally, the TAP -Therapeutic Antibody Profiler- is also an interactive molecular viewer allowing users to explore surface features such as hydrophobicity, charge distribution, and potential sequence liabilities. Additionally, it offers an estimate of the model's quality to support result interpretation, and it automatically identifies the canonical forms of all non-CDRH3 loops [19].

Results and discussion

A comprehensive analysis was conducted to evaluate docking results, binding patterns, including hydrogen bonds, non-bonded contacts and salt bridges. This analysis was extended to assess some crucial aspects of antibody developability, i.e. its predicted allergenicity, immunogenicity/antigenicity, stability, half-life, and its therapeutic profile. **Table 1** shows molecular docking results conducted via ClusPro to investigate the intricate effects of sequential and cumulative alteration on the binding affinity of a protein complex. The analysis exclusively concentrated on Cluster 0 for all analyses, a decision driven by its consistent representation of the highest number of members across all docking results. This study involves a direct comparison between the binding affinity of the wild-type protein (Non-Modified (STD)) and a set of modifications that were introduced step by step. The binding affinity was measured in kcal/mol, where more negative values indicate a stronger and more stable interaction between molecules. The analysis was started by the wild-type protein STD with a binding affinity of (- 766.5 kcal/mol). The first pair of modifications were tyrosine (Tyr) in position 53, replaced with arginine (Arg) in chain H, and serine (Ser) in position 93 replaced with isoleucine (Ile), indicating a marked improvement in the binding affinity of - 944.3 kcal/mol. However, the next two pairs of modifications show notable deteriorations in their binding affinity. The glycine (Gly102) changed to cystine (Cys) in chain H, and tyrosine (Tyr92) changed to phenylalanine (Phe) in chain L, reducing the binding affinity to 701.2 kcal/mol. Tyrosine (Tyr107) replaced

with tryptophan (Trp) in chain H and tyrosine (Tyr32) replaced with arginine (Arg) in chain L resulted in a binding affinity of - 764.7kcal/mol. In contrast to the previous two pairs of modifications, the remaining substitutions improved the binding affinity; however, the last set of substitutions shows the best binding affinity of - 945.9 kcal/mol among all sets.

Table 1: Molecular docking results obtained using ClusPro, showing the effect of sequential amino-acid substitutions on protein-protein binding affinity

		Modification		
Cluster	**Members**	**Chain H**	**Chain L**	**Center score kcal/mol**
0	118	No Modifications (STD)		- 766.5
0	170	Tyr53 to Arg	Ser93 to Ile	- 944.3
0	116	Gly102 to Cys	Tyr92 to Phe	- 701.2
0	107	Tyr107 to Trp	Tyr32 to Arg	- 764.7
0	099	Asn57 to Met	Thr94 to Arg	- 816.4
0	109	Tyr106 to Lys	Asn30 to Gln	- 825.2
0	105	Lue105 to His	Tyr91 to Phe	- 862.8
0	125	Tyr110 to Phe	Ser31 to Gln	- 867.8
0	123	Tyr108 to Phe	Gln30 to Ile	- 903.9
0	142	Trp52 to Phe	Arg32 to His	- 815.5
0	116	Cys101 to val50	Ala50 to Val	- 945.9

Analysis was limited to Cluster 0, which consistently contained the highest number of members. Binding affinities are reported in kcal/mol, with more negative values indicating stronger interactions. Compared with the wild-type protein (STD; - 766.5 kcal/mol), initial substitutions enhanced binding affinity, whereas intermediate modifications reduced it. Subsequent substitutions improved binding, with the final modification set exhibiting the strongest affinity (- 945.9 kcal/mol)

Positive impact (improved affinity): A study introducing mutations across CDRs of 21 monoclonal antibodies (mAbs) found that 38 substitutions in 21 CDR positions improved binding affinity by up to 870-fold. For example, replacing Gly102 with Cys in CDR-H3 optimized hydrophobic interactions, leading to stronger antigen binding [20, 21]. Introducing a YSLLL-motif in the CDR3 loop of shark IgNAR antibodies improved affinity by10-fold due to slower off-rates [22].

Negative impact (reduced affinity): In cetuximab Fab complexes, replacing hydrophobic residues (Phe3→His) reduced affinity by disrupting hydrophobic packing [23]. Substituting arginine with citrulline (neutral) at positions 8 and 9 in meditope-Fab complexes abolished salt bridges, reducing affinity by >10-fold [23]. The studies confirm that amino acid substitution in the Fab, especially in the CDR region have a significant impact on modulating binding affinity. The results are provided in the **Table1**, aligned with these principles, like substitution of tyrosine in position 59 in chain H with arginine and serine in chain L position 93 with isoleucine, improved the center score (- 944.3 vs - 799.5) by adding charged and hydrophobic residues.

Table 2 elucidates the summary of the amino acid residues involved in the interaction between chain B, representing the CTLA4 receptor, and modified drug chains H and L. Compared with the wild-type (STD in the wild-type) complex, the interaction between chain B and chain H involved 15: 14 amino acid residues, with an interface area of 608: 645 $Å^2$. This interaction was stabilized with one salt bridge, 10 hydrogen bonds, and 103 non-bonded contacts (hydrophobic interactions, *van der Waals* forces). Alternatively, chain B was engaged with chain L via 8: 4 amino acid residues, respectively, covering an interface area of 334: 360 $Å^2$, supported by 3 hydrogen bonds, and 55 non-bonded contacts. In the first set of substitutions (Arg53 and Ile93), the number of interacting residues between chain B and chain H increased to 18, respectively. This incremented to an expansion

of the interface area to 638: 710 Å^2, and improved the complex stability through the formation of 3 salt bridges, 9 hydrogen bonds, and 122 non-bonded contacts. The impact of this pair of substitutions led to an increment in the number of interacting residues to 8: 7. At a decrease in the interface area to 311: 327 Å^2, the complex stabilized with 3 hydrogen bonds and 50 non-bonded contacts between chain B and chain L. The other sets of substitutions showed a variety of results and effects on the interacted residues, interface area (Å^2), Salt bridges and hydrogen bonds. However, the last set of substitution showed a decline in the interacted residues to 9: 9, the interface area to 481: 528, and a notable decline in the hydrogen bonds, non-bonded contacts 5 and 57, for chain B and H, respectively. In contrast, the impact of this set showed an increment of the interacted residues to 11: 10, an expansion of the interface area to 458: 506, and improvement in complex stability, which was stabilized by 7 hydrogen bonds, 63 non-bonded contacts, for chain B and L of the last set. In SARS-CoV-2 antibodies, computational redesign of Fab CC12.3 increased salt bridges in CDR-L1/L3, improving predicted binding affinity beyond ACE2 [24]. Crystal structures show native antibody-antigen complexes have 7.7 ± 3.3 hydrogen bonds, while engineered models average only 3.0 ± 1.5, explaining weaker binding [25]. Hydrophobic interactions account for 50.0 - 70.0% of binding energy in antibody-antigen complexes [26].

Table 2: Amino-acid interactions between chain B (CTLA4) and drug chains H and L for the wild-type (STD) and modified complexes

No.	Receptor chain B: Drug chain H						Receptor chain B: Drug chain L					
	Interacted residues	Interface Area (Å^2)	Salt Bridges	Disulfide bonds	Hydrogen bonds	Non-bonded Contacts	Interacted residues	Interface area (A^2)	Salt Bridges	Disulfide Bonds	Hydrogen Bonds	Non-bonded contacts
STD	15: 14	608: 645	1	-	10	103	8: 4	334: 360	-	-	3	55
Arg53 Ile93	18: 13	638: 710	3	-	9	122	8: 7	311: 327	-	-	4	50
Cys102 Phe92	12: 09	538: 571	2	-	4	76	6: 4	289: 304	-	-	4	42
Trp107 Arg32	16: 11	588: 663	3	-	8	106	6: 4	330: 363	-	-	6	37
Met57 Arg94	16: 12	594: 651	3	-	9	97	10: 8	382: 416	-	-	3	64
Lys106 Gln30	16: 13	638: 685	3	-	10	94	10: 8	396: 433	-	-	3	68
His105 Phe91	20: 14	666: 738	3	-	12	139	7: 6	356: 381	-	-	4	48
Phe110 Gln31	19: 14	666: 750	3	-	12	130	7: 6	351: 357	-	-	4	47
Phe108 Ile30	17: 12	621: 699	2	-	9	105	7: 5	358: 377	-	-	4	46
Phe52 His32	10: 08	488: 516	1	-	4	60	12: 7	422: 470	-	-	7	60
Cys101 Val50	09: 09	481: 528	1	-	5	57	11: 10	458: 506	-	-	7	63

This presents interacting residues, interface area (Å²), and stabilizing interactions (salt bridges, hydrogen bonds, and non-bonded contacts). Amino-acid substitutions produced variable effects, with early modifications enhancing chain B-H interactions, while the final substitution reduced chain B-H contacts but strengthened chain B-L interactions

Table 3 provides the allergenic potential of antibody chains and the immunologic response of the wild-type and the 10 consecutive pairs of modifications. To evaluate the allergenic potential of the antibody chains, the heavy (H) and light (L) chains were analyzed in their standard and modified forms using the AlgPred server. This tool applies to several approaches, including machine learning (ML), motif-based detection via MERCI, sequence alignment through BLAST, and an overall hybrid score that combines all outputs. The final result - either Allergen or Non-allergen - is based on the integration of these scores as shown the ST chains labeled as allergen where they scored via ML score (0.48) (0.36), MERCI score (0.5) (0.0), BLAST score (0.5) (0.0), and hybrid score

(1.48) (0.36) for chain H and L, respectively. As noted, the chain H was labeled as an allergen with varied values, where the 9th set (Phe 52, His 32) gave the lowest value among all sets. In contrast the chain L revealed that the 1st (Arg53, Ile93), 2nd (Cys102, Phe92), 7th (Phe110, Gln31), 8th (Phe108, Ile30), and the 9th (Phe52, His32) sets labeled as allergen, while the 3rd (Trp107, Arg32), 4th (Met57, Arg94), 5th (Lys106, Gln31), 6th (His105, Phe91), and the 10th (Cys101, Val50) sets labeled as non-allergen. The sets were found to be scored less than the ST, were the 3rd (Trp107, Arg32) chains H and L scores were ML (0.45) (0.36), MERCI (0.5) (0.0), BLAST (0.5) (- 0.5), and hybrid (1.45) (- 0.16). For the 4th set (Met57, Arg94) chains H and L scores were ML (0.42) (0.31), MERCI (0.5) (0.0), BLAST (0.5) (- 0.5), and hybrid (1.42) (-0.19), 5th modified set (Lys106, Gln30) chains scored as followed, ML (0.44) (0.31), MERCI (0.5) (0.0), BLAST (0.5) (-0.5), and hybrid (1.44) (- 0.19), for 6th set (His105, phe91) the scoring function were: ML (0.44) (0.31), MERCI (0.5) (0.0), BLAST (0.5) (- 0.5), and hybrid (1.43) (- 0.18). The 10th (Cys101, Val50) set was found to have a higher result compared to the STD regarding the chain H. To the scoring function were as following: ML (0.51) (0.31), MERCI (0.5) (0.0), BLAST (0.5) (- 0.5), hybrid (1.51) (- 0.19) and the 9th set gave the best scores among all the sets. The prediction of allergenic potential is crucial to ensure safety, due to the rapid increase in protein application. They are used in therapeutics, food, household products, and pharmaceuticals [27]. Innovations in protein engineering can help redesign allergenic proteins to reduce adverse reactions in sensitive individuals. To accomplish this, a comprehensive understanding of the molecular properties and features that confer allergenicity to proteins is essential [28]. **Table 3** shows the average antigenic propensity; the STD score was 1.0413. Scores were found to give a slight variation from the STD. The second and the tenth had higher scores than the STD, while the other sets showed values less than STD, except for the nineth which had exactly the same value as STD. Notably, set number 7 gave 1.0401 which is considered the best among all. Protein-based therapeutics may exhibit undesired immune responses in a subset of patients, leading to the production of antidrug antibodies. In some cases, antidrug antibodies have been reported to affect the pharmacokinetics, efficacy, and/or safety of the drug [29]. As a result, numerous approaches have been developed to assess the immunogenicity risk of biologics using *in silico* and *in vitro* methods [30].

Table 1: *In silico* evaluation of allergenic potential and immunogenicity of the wild-type (STD) and consecutively modified antibody heavy (H) and light (L) chains

	AlgPred										Immunomedicine group
	ML score		MERCI score		BLAST score		Hybrid score		Prediction score		Average antigenic propensity
STD	H	L	H	L	H	L	H	L	H	L	
	0.48	0.36	0.5	0.0	0.5	0.0	1.48	0.36	Allergen	Allergen	1.0413
Arg53 Ile93	0.44	0.37	0.5	0.0	0.5	0.0	1.44	0.37	Allergen	Allergen	1.0409
Cys102 Phe92	0.45	0.36	0.5	0.0	0.5	0.0	1.45	0.36	Allergen	Allergen	1.0420
Trp107 Arg32	0.45	0.36	0.5	0.0	0.5	- 0.5	1.45	- 0.16	Allergen	Non-allergen	1.0407
Met57 Arg94	0.42	0.31	0.5	0.0	0.5	- 0.5	1.42	- 0.19	Allergen	Non-allergen	1.0408
Lys106 Gln30	0.44	0.31	0.5	0.0	0.5	- 0.5	1.44	- 0.19	Allergen	Non-allergen	1.0408
His105 Phe91	0.43	0.32	0.5	0.0	0.5	- 0.5	1.43	- 0.18	Allergen	Non-allergen	1.0403
Phe110 Gln31	0.44	0.32	0.5	0.0	0.5	0.0	1.42	0.32	Allergen	Allergen	1.0401
Phe108 Ile30	0.42	0.32	0.5	0.0	0.5	0.0	1.42	0.32	Allergen	Allergen	1.0403
Phe52 His32	0.41	0.32	0.5	0.0	0.5	0.0	1.41	0.32	Allergen	Allergen	1.0413
Cys101 Val50	0.51	0.31	0.5	0.0	0.5	- 0.5	1.51	- 0.19	Allergen	Non-allergen	1.0433

Allergenicity was predicted using the AlgPred server based on machine learning, MERCI motifs, BLAST alignment, and hybrid scores, while average antigenic propensity was also reported. The modifications produced variable effects on allergenicity and immunogenicity, with several substitution sets reducing scores compared with the STD. Overall, selected variants showed improved safety-related profiles relative to the wild-type antibody

Table 4 showed that STD and all the modified sets exhibit identical half-lives, assessed in three different biological systems: mammalian reticulocytes *in vitro*, yeast *in vivo* and *E. coli in vivo*; the results were elicited at 0.8 hr., 10 min, and 10 hr., respectively. On the other hand, the instability index for the STD and all sets of substitutions exhibited as 94.06, 48.52, 48.62, 48.26, 48.15, 49.22, 49.96, 48.85, 48.88, 48.88, and 48.33, respectively, which are all classified as unstable, despite the slight improvement shown in some of these modified sets. The estimated half-life is determined by the N-terminal amino acid sequence under investigation. The half-life is the prediction of the time it takes for half of the amount of protein in a cell to disappear after its synthesis in the cell. The prediction is given for three organisms (human, yeast, and *E. coli*), but it is possible to extrapolate the result to similar organisms. A stability index value over 40 indicates that the investigated protein may be unstable, while a value less than 40 is stable [16]. As shown in **Figures 2-6** for the total CDR length, the STD and all modified versions exhibit identical values of 52. Regarding the CDR vicinity PSH score, the STD and modified sets yield values of 121.53, 129.3421, 153.3187, 158.023, 153.7158, 153.7603, 156.3226, 146.0911, 159.2098, 157.5302, and 150.1099, respectively, for the CDR vicinity PPC score, the STD exhibit a value of 0.0434, while all of the modified versions show values of 0.0886, 0.0999, 0.1173, 0.3434, 0.2877, 0.4968, 0.3841, 0.4634, 0.4424, and 0.1873, respectively. Furthermore, for the CDR vicinity PNC and SFvCSP scores, the results of the STD and modified sets presents values of 0.1104 and 15.0 for PNC and SFvCSP, respectively, while the modified sets display values of (0.0962, 18.0), (0.0825,15.0), (0.094, 20.0), (0.0932, 25), (0.1637,25.0), 0.1588, 25.5), (0.1774, 25.5), (0.0608, 30.5), (0.0611, 25.01), and (0.0938, 20.91) for each, respectively. Based on the acceptable ranges for these properties [17], all obtained results fall in acceptable criteria. However, a detailed comparison reveals that the STD generally demonstrates more favorable outcomes across most parameters, compared with all sets, which makes all the sets have favorable developability. Therapeutic Antibody Profiler is designed to identify antibodies that possess characteristics that are rare/unseen in clinical-stage mAb therapeutics. This is particularly relevant given that hydrophobicity within the Complementarity Determining Regions (CDRs) has been consistently linked to aggregation propensity in monoclonal antibodies (mAbs). Furthermore, surface patches of positive and negative charge have been implicated in undesirable biophysical characteristics. Specifically, mAbs exhibiting oppositely charged heavy (VH) and light (VL) chains typically demonstrate elevated *in vitro* viscosity values, higher rates of clearance, and suboptimal expression levels. Equally, asymmetry in the net charge of the heavy- and light-chain variable domains correlates with increased self-association and viscosity at high concentrations [17].

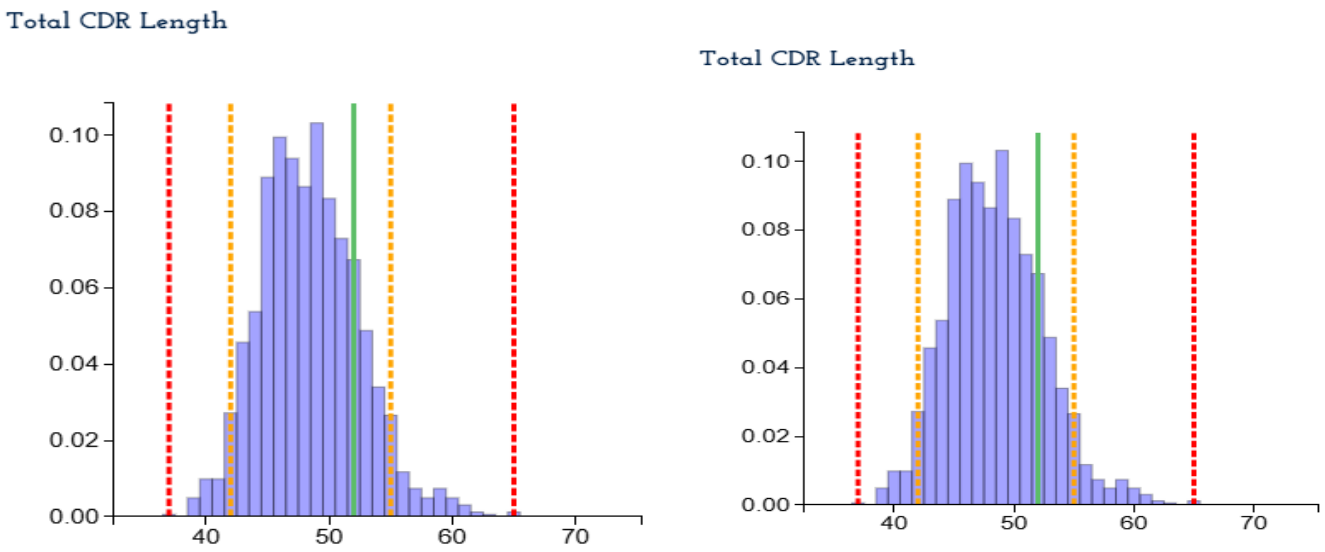

Figure 2: Total CDR length of STD and modified version -last set: contain all sets -

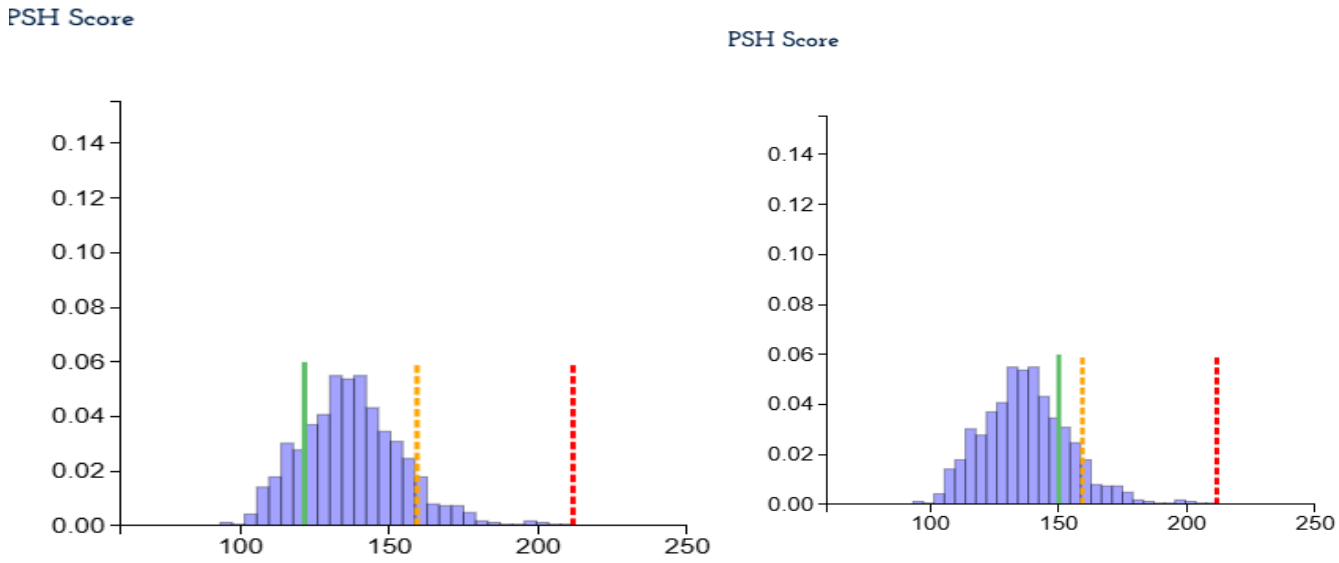

Figure 3: PSH score for STD and modified version -last set: contain all sets -

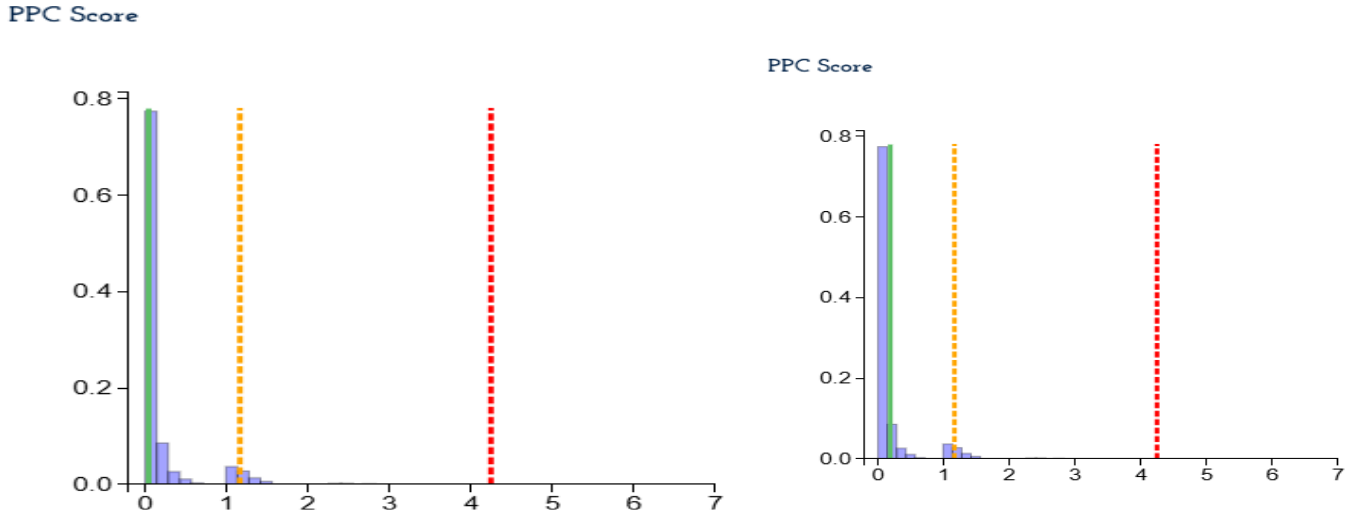

Figure 4: PPC score for STD and modified version -last set: contain all sets -

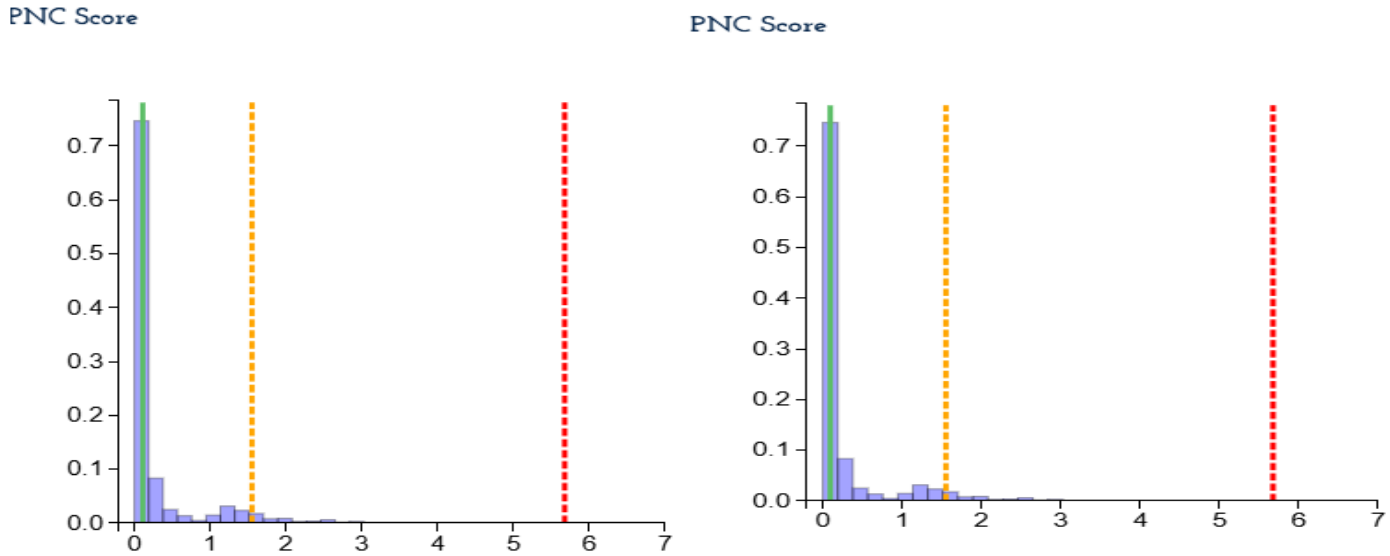

Figure 5: PPC Score for STD and modified version -last set: contain all sets -

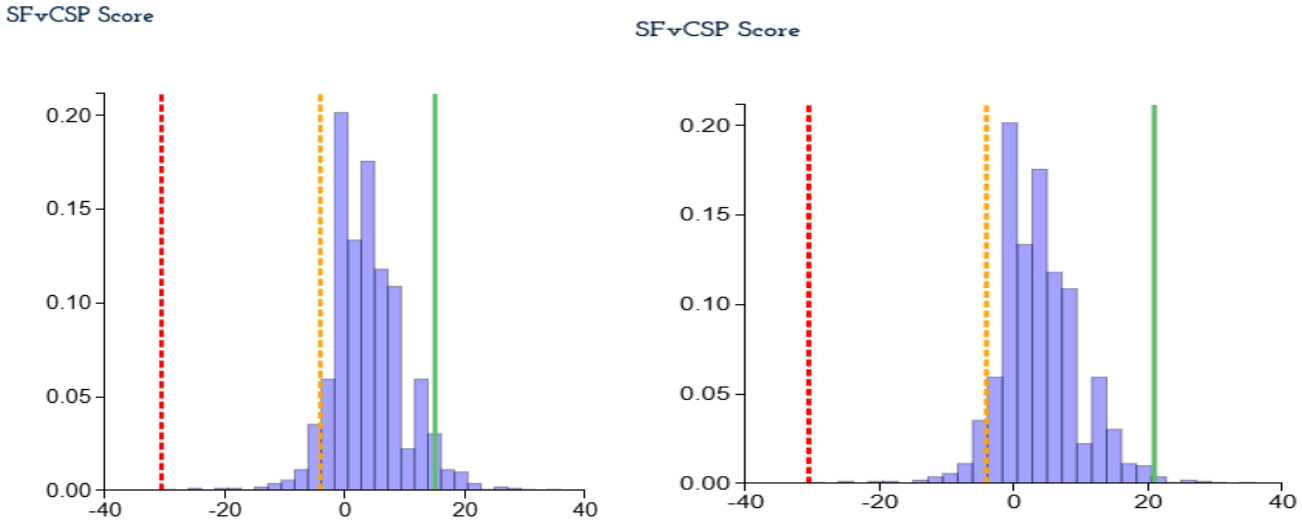

Figure 6: SFvCSP score for STD and (modified version-last set: contains all sets -

These figures show the properties of the STD and the final version of medications, which contain all the previous modification sets, as mentioned before,where estimated from TAP. This is because the study focused mainly on improving the binding affinity, which this condition complies with.

Table 4: Developability assessment of the wild-type (STD) and modified antibody variants

	Protparm				TAP				
	Half-life								
STD	Mammalian reticulocytes *in-vitro*	Yeast *in-vivo*	E. coli *in-vivo*	Instability index	Total CDR length	CDR vicinity PSH score (kyteanddoo little)	CDR vicinity PPC score	CDR vicinity PNC score	SFvCSP score
	0.8 hr.	10 min	10 hr.	49.06 unstable	52	121.53	0.0434	0.1104	15.0
Arg53 Ile93	0.8 hr.	10 min	10 hr.	48.52 unstable	52	129.3421	0.0886	0.0962	18.0
Cys102 Phe92	0.8 hr.	10 min	10 hr.	48.62 unstable	52	153.3187	0.0999	0.0825	15.0
Trp107 Arg32	0.8 hr.	10 min	10 hr.	48.26 unstable	52	158.023	0.1173	0.094	20.0
Met57 Arg94	0.8 hr.	10 min	10 hr.	48.15 unstable	52	153.7158	0.3434	0.0932	25.0
Lys106 Gln30	0.8 hr.	10 min	10 hr.	49.22 unstable	52	153.7603	0.2877	0.1637	25.0
His105 Phe91	0.8 hr.	10 min	10 hr.	49.96 unstable	52	156.3226	0.4968	0.1588	25.5
Phe110 Gln31	0.8 hr.	10 min	10 hr.	48.85 unstable	52	146.0911	0.3841	0.1774	25.5
Phe108 Ile30	0.8 hr.	10 min	10 hr.	48.88 unstable	52	159.2098	0.4634	0.0608	30.5
Phe52 His32	0.8 hr.	10 min	10 hr.	48.88 unstable	52	157.5302	0.4424	0.0611	25.01
Cys101 Val50	0.8 hr.	10 min	10 hr.	48.33 unstable	52	150.1099	0.1873	0.0938	20.91

All variants exhibited identical predicted half-lives in mammalian reticulocytes, yeast, and *E. coli*. Instability indices classified the STD and all modified sets as unstable, with minor variations among substitutions. CDR length, CDR vicinity scores, and therapeutic antibody profiler parameters were within acceptable ranges for all variants. Overall, while the STD showed slightly more favorable values across several metrics, all modified sets met the developability criteria

Conclusion: This study investigates the impact of specific modifications on the binding interaction between CTLA4 and Tremelimumab, by employing molecular docking. On the other hand, this could improve the binding affinity and increase complex stability, as shown in the cumulative alteration number 10 (Arg101 to Cys/ Ala50 to Val, where binding affinity is equal to - 945.9 kcal/mole). These divergent outcomes highlight the critical sensitivity of the antibody-antigen interface to amino acid changes, underscoring the delicate balance required for optimal therapeutic binding. The ability to identify specific modifications that either enhance or diminish binding affinity provides invaluable molecular-level insights into the determinants of Tremelimumab's efficacy. Such findings are paramount for guiding rational drug design, allowing for the targeted optimization of antibody characteristics to achieve desired pharmacological profiles. The Tremelimumab demonstrated susceptibility to further optimization in its binding affinity through targeted modifications, with some improvement in its developability properties, and some regression in other properties.

References

1. Bray F, Laversanne M, Sung H, Ferlay J, Siegel RL, Soerjomataram I, et al. Global cancer statistics 2022: GLOBOCAN estimates of incidence and mortality worldwide for 36 cancers in 185 countries. CA Cancer Journal Clinical. 2024; 74(4): 229-263. doi: 10.3322/caac.21834
2. O'Donnell-Tormey J, Matthew Tontonoz M. Cancer and the immune system: The vital connection. 1987; Cancer Research Institute, 29 Broadway, York, NY, USA.
3. Alhadi AM, Alhadi AM, Mame ME, Mohammed AA, Ali AA. Evaluation of genetic engineering tools in anticancer drug discovery: Evidence-based insights for Libyan Pharmacology Departments. Mediterranean Journal of Pharmacy and Pharmaceutical Sciences. 2025; 5(4): 21-28. doi: 10.5281/zenodo.17334913
4. Minda AG, Awel FS, Seifudin KA, Gezahegne MK. Immunotherapy against cancer: A comprehensive review. Journal of Cancer Research and Experimental Oncology. 2016; 8(2): 15-25. doi: 10.5897/JCREO2015.0124
5. Carter BW. Immunotherapy in lung cancer and the role of imaging. Seminars in Ultrasound, CT and MRI39. 2018; 39(3): 314-321. doi: 10.1053/j.sult.2028.02.004
6. France NL, Blair HA. Tremelimumab: A review in advanced or unresectable hepatocellular carcinoma. Targeted Oncology. 2024; 19(1): 115-123. doi: 10.1007/s11523-023-01026-9
7. Tarhini AA, Kirkwood JM. Drug evaluation Tremelimumab (CP-675,206): A fully human anticytotoxic T lymphocyte-associated antigen 4 monoclonal antibody for treatment of patients with advanced cancers. Expert Opinion on Biological Therapy. 2008; 8(10): 1583-1593 doi: 10.1517/14712598.8.10.1583
8. France NL, Blair HA. Tremelimumab: A review in advanced or unresectable hepatocellular carcinoma. Targeted Oncology. 2024; 19(1): 115-123. doi: 10.1007/s11523-023-01026-9
9. Garon EB, Cho BC, Luft A, Alatorre-Alexander J, Geater SL, Trukhin D, et al. A brief report of Durvalumab with or without Tremelimumab in combination with chemotherapy as first-line therapy for metastatic non-small-cell lung cancer: Outcomes by Tumor PD-L1 Expression in the Phase 3 POSEIDON Study. Clinical of Lung Cancer. 2024; 25(3): 266-273.e5. doi: 10.1016/j.cllc.2024.03.003
10. Bittrich S, Bhikadiya C, Bi C, Chao H, Duarte JM, Dutta S, et al. RCSB protein data bank: Efficient searching and simultaneous access to one million computed structure models alongside the Pdb structures enabled by architectural advances. Journal of Molecular Biology. 2023; 435(14): 167994. doi: 10.1016/j.jmb.2023.167994
11. Yuan S, Chan HCS, Hu Z. Using PyMOL as a platform for computational drug design. Wiley Interdisciplinary Reviews: Computational Molecular Science. 2017; 7(2): e1298. doi: 10.1002/wcms.1298
12. Laskowski RA. Enhancing the functional annotation of PDB structures in PDBsum using key figures extracted from the literature. Bioinformatics. 2007; 23(4): 1824-1827. doi: 10.1093/bioinformatics/btm085
13. Gbaj AM, Sherif FM. Gene mutations and pharmacogenetics. Pharmacy and Pharmacology International Journal. 2016; 4(4): 00085. doi: 10.15406/ppij.2016.04.00085
14. Alharati SH, Elbakay JAM, Hermann A, Gbaj AM. Polycystic ovary syndrome: Molecular modeling study on potential Lepidium sativum bioactive compounds in modulating kiss-1 gene function. Mediterranean Journal of Medical Research. 2025; 2(3): 129-140. doi: 10.5281/zenodo.17069661
15. Kozakov D, Hall DR, Xia B, Porter KA, Padhorny D, et al. The ClusPro web server for protein-protein docking. Nature Protocols. 2017; 12(2): 255-278. doi: 10.1038/nprot.2016.169

16. Hoque F, Nahar N, Annie FS, Rahim A, Hossain MK, Abdul Rahman MN, et al. Synthesis, characterization and complexation of Schiff base ligand p-anisalcefuroxime with Cu^{2+} and Fe^{2+} ions; antimicrobial and docking analysis with PBP2xto study pharmacokinetic parameters. Mediterranean Journal of Pharmacy and Pharmaceutical Sciences. 2025; 5(1): 48-64. doi: 10.5281/zenodo.14647651
17. Saha S, Raghava GPS. AlgPred: Prediction of allergenic proteins and mapping of IgE epitopes. Nucleic Acids Research. 2006; 34: W202-W209. doi: 10.1093/nar/gkl343
18. Saivish MV, Menezes GL, Costa VGD, Silva GCDD, Marques RE, Nogueira ML, Silva RAD. Predicting antigenic peptides from Rocio virus NS1 protein for immunodiagnostic testing using immunoinformatic and molecular dynamics simulation. International Journal of Molecular Sciences. 2022; 23(14): 7681. doi: 10.3390/ijms23147681
19. Wilkins MR, Gasteiger E, Bairoch A, Sanchez JC, Williams KL, Appel RD, Hochstrasser DF. Protein identification and analysis tools in the ExPASy server. Methods in Molecular Biology. 1999; 112: 531-552. doi: 10.1385/1-59259-584-7:531
20. Raybould MIJ, Marks C, Krawczyk K, Taddese B, Nowak J, Lewis AP, et al. Five computational developability guidelines for therapeutic antibody profiling. Proceeding National Academy of Sciences of the USA. 2019; 116(10): 4025-4030. doi: 10.1073/pnas.1810576116
21. Rajpal A, Beyaz N, Haber L, Cappuccilli G, Yee H, Bhatt RR, et al. A general method for greatly improving the affinity of antibodies by using combinatorial libraries. Proceedings of the National Academy of Sciences of the United States of America. 2005; 102(24): 8466-8471. doi: 10.1073/pnas.0503543102
22. Nuttall SD, Humberstone KS, Krishnan UV, Carmichael JA, Doughty L, Hattarki M, et al. Selection and affinity maturation of IgNAR variable domains targeting Plasmodium Falciparum AMA1. Proteins. 2004; 55(1): 187-197. doi: 10.1002/prot.20005
23. Bzymek KP, Avery KA, Ma Y, Horne DA, Williams JC. Natural and non-natural amino-acid side-chain substitutions: Affinity and diffraction studies of meditope-Fab complexes. Acta Crystallographica Section: F Structural Biology Communications. 2016; 72(11): 820-830. doi: 10.1107/S2053230X16016149
24. Treewattanawong W, Sitthiyotha T, Chunsrivirot S. Computational redesign of Fab CC12.3 with substantially better predicted binding affinity to SARS-CoV-2 than human ACE2 receptor. Scientific Reports. 2021; 11(1): 15476. doi: 10.1038/s41598-023-42442-1
25. Kilambi KP, Gray JJ. Structure-based cross-docking analysis of antibody-antigen interactions. Scientific Reports. 2017; 7(1): 8145. doi: 10.1038/s41598-017-08414-y
26. González-Muñoz A, Bokma E, O'Shea D, Minton K, Strain M, Vousden K, Rossant C, et al. Tailored amino acid diversity for the evolution of antibody affinity. Monoclonal antibodies. 2012; 4(6): 664-672. doi: 10.4161/mabs.21728
27. Garcia-Moreno FM, Gutiérrez-Naranjo MA. Allerdet: A novel web app for prediction of protein allergenicity. Journal of Biomedical Informatics. 2022; 135: 104217. doi: 10.1016/j.jbi.2022.104217
28. Yang C, Negi SS, Schein CH, Braun W, Kim P. Allergen AI: A deep learning model predicting allergenicity based on protein sequence. bioRxiv: The preprint server for Biology. 2024; doi: 10.1101/2024.06.22.600179
29. Hu Z, Wu P, Swanson SJ. Evaluating the immunogenicity risk of protein therapeutics by augmenting T cell epitope prediction with clinical factors. The American Association of Pharmaceutical Scientists Journal. 2025; 27(1): 33. doi: 10.1208/s12248-024-01003-8
30. Mattei AE, Gutierrez AH, Seshadri S, Tivin J, Ardito M, Rosenberg AS, et al. *In silico* methods for immunogenicity risk assessment and human homology screening for therapeutic antibodies. Monoclonal Antibodies. 2024; 16(1): 2333729. doi: 10.1080/19420862.2024.2333729

Author contribution: AMG conceived, designed the study. NAI collected data. NAI, HAG, MAG & AH contributed to data analysis. NAI, AH & AMG performed and interpreted the analysis. NAI & AMG drafted the manuscript. All authors agreed to be accountable for its contents.
Conflict of interest: The authors declare the absence of any commercial or financial relationships that could be construed as a potential conflict of interest.
Ethical issues: The authors completely observed ethical issues, including plagiarism, informed consent, data fabrication or falsification, and double publication or submission.
Data availability statement: The raw data that support the findings of this article are available from the corresponding author upon reasonable request.
Author declarations: The authors confirm that they have followed all relevant ethical guidelines and obtained any necessary IRB and/or ethics committee approvals.
Generative AI disclosure: No generative AI was used in the preparation of this manuscript.